Journal of Materials Chemistry C

Accepted Manuscript

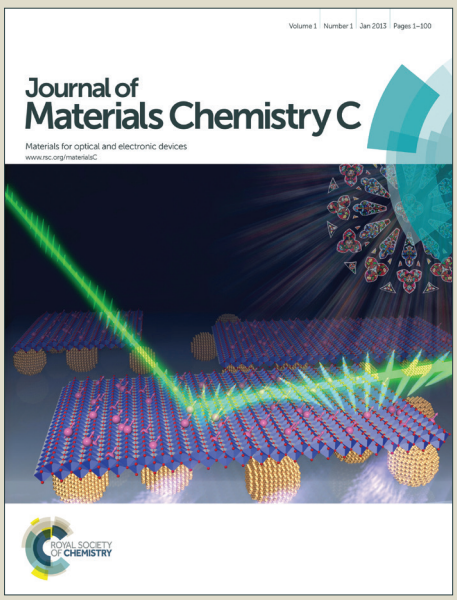

ROYAL SOCIETY OF CHEMISTRY

www.rsc.org/materialsC

Cite this: DOI: 10.1039/c0xx00000x

www.rsc.org/xxxxxx

COMMUNICATION

Covalently Grafting Nonmesogenic Moieties onto Polyoxometalate for Fabrication of Thermotropic Liquid-Crystalline Nanomaterials

Chang-Gen Lin, Wei Chen, Solomon Omwoma, and Yu-Fei Song*[a]

Received (in XXX, XXX) Xth XXXXXXXXX 20XX, Accepted Xth XXXXXXXXX 20XX

DOI: 10.1039/b000000x

We demonstrated herein the first class of polyoxometalate-containing thermotropic liquid-crystalline materials, in which the nonmesogenic organic moieties were covalently tethered onto the nanoscaled polyoxometalate. These materials showed layered smectic A (SmA) phase when cooling from isotropic state.

Liquid crystal (LC) state exists between the crystalline solid and the amorphous liquid.[1] Combining both order and mobility, liquid crystals exhibit anisotropic and switching properties that are conducive to numerous applications.[2] In the past decade, there has been an increasing interest in the field of liquid crystal nanoscience, which primarily deals with the synergetic relationship between LCs and nanomaterials such as nanoparticles and nanotubes.[3] Nanomaterials can introduce specific characteristics into LC systems and enhance the physical properties of LCs, while LCs provide a very good support for the self-assembly of nanomaterials into well-defined functional superstructures in multiple dimensions.[4] Polyoxometalates (POMs) are a class of discrete anionic metal oxides with intriguing physical properties and unmatched range of structures that can range in size from nano to micrometer scale.[5] Incorporation of the nanoscaled POMs into LCs generates novel functional liquid-crystalline nanomaterials and has received increasing attention over recent years.[6-8] A widely used method to fabricate liquid-crystalline POM nanomaterials is the encapsulation of POM anions into mesogenic or nonmesogenic cationic surfactants.[7] However, few examples based on the covalent modification have been reported,[8] although the covalent approach indeed offers indisputable assets.[9]

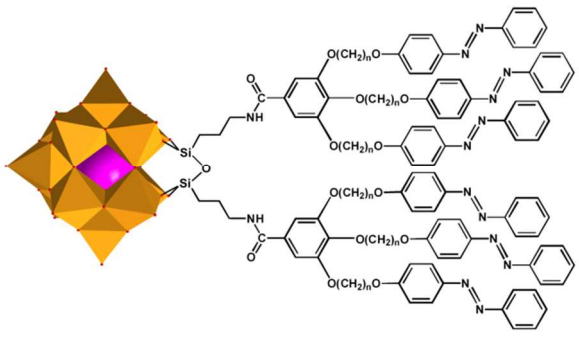

Scheme 1 A schematic presentation of liquid-crystalline polyoxometalate hybrids **1a-c** (a, n = 8; b, n = 10; c, n = 12) with WO_6 as gold octahedron and SiO_4 as pink sphere.

In the search of POM-based advanced functional materials, herein we present the fabrication of liquid-crystalline nanomaterials based on $[(C_4H_9)_4N]_4[(SiW_{11}O_{39})O\{Si(CH_2)_3\text{-}NH_2\bullet HCl\}_2]$ (**SiW_{11}-NH_2**) Keggin POM cluster (Scheme 1). The synthetic procedure is straightforward and consists of a one-step reaction of **SiW_{11}-NH_2** with gallic acid derivatives that have been applied to obtain thermotropic mesophases with single-molecule magnets, octahedral metal atom clusters *etc.*[10-12]

The gallic acid derivatives were synthesized with long alkyl chains bearing azobenzene groups, which are widely used as rigid units in the fabrication of liquid-crystalline materials. In our case, differential scanning calorimetry (DSC) and optical polarized microscopy (OPM) experiments showed that the gallic acid derivatives did not show liquid-crystalline properties (See supporting information). Grafting these gallic acid derivatives onto POM clusters through amide bonds gave rise to compounds **1a-c**.

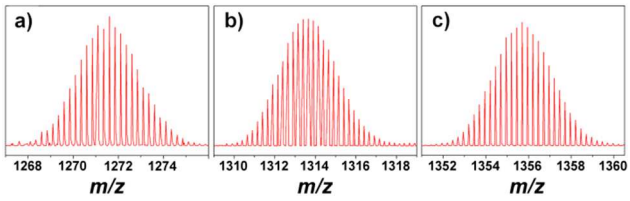

Fig. 1 a) ESI-MS spectrum of **1a** with peaks at *m/z* 1271.35; b) ESI-MS spectrum of **1b** with peaks at *m/z* 1313.39; c) ESI-MS spectrum of **1c** with peaks at *m/z* 1355.70. The ESI-MS spectrometer was calibrated by using 5mM HCOONa solution (2-propanol/H_2O = 90/10).

The molecular structures and conformations of **1a-c** were investigated by different techniques. FT-IR spectra of **1a-c** show typical amide C=O stretching vibrations at ca. 1660 cm^{-1}, and characteristic **SiW_{11}-NH_2** stretching vibrations at ca. 1044 (Si-O-Si), 965 (W=O), and 850 (W-O-W) cm^{-1}, indicating gallic acid derivatives have been grafted onto POMs. In the ^1H NMR spectra of **1a-c**, signals of the tetrabutylammonium cation and the gallic acid derivative are clearly observed and fit well with the molecular structures. The ^{29}Si NMR spectra of **1a-c** show two signals at ca. -52 ppm and -85 ppm, which can be assigned to the Si in the silane and the heteroatom of the mono-lacunary Keggin cluster of SiW_{11}, respectively (Fig. S7-9). Although the above analytical methods gave a good indication for the formation of the desired compounds, electrospray ionization mass

spectrometry (ESI-MS) provided further convincing structural information. ESI-MS spectra of **1a-c** show several intense signals characterized by complex isotope patterns (Fig. S10-12). It is possible to assign all the signals (Table S2-4). For example, ESI-MS peaks of **1a** observed at *m/z* 1271.35 can be attributed to $\{[(SiW_{11}O_{40})\{Si(CH_2)_3NHCOC_6H_2(OC_8H_{16}OC_{12}H_9N_2)_3\}_2]+HCO ONa\}^{4-}$ (Fig. 1a), while peaks of **1b** observed at *m/z* 1313.39 correspond to $\{[(SiW_{11}O_{40})\{Si(CH_2)_3NHCOC_6H_2(OC_{10}H_{20}OC_{12}H_9N_2)_3\}_2]+HCOONa\}^{4-}$ (Fig. 1b). In the case of **1c**, ESI-MS peaks observed at *m/z* 1355.70 can be assigned to $\{[(SiW_{11}O_{40})\{Si(CH_2)_3NHCOC_6H_2(OC_{12}H_{24}OC_{12}H_9N_2)_3\}_2]+HCOONa\}^{4-}$ (Fig. 1c).

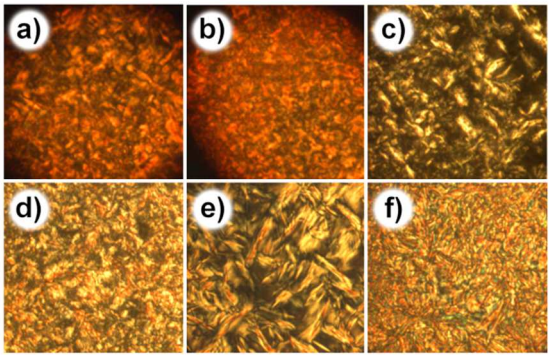

Fig. 2 Optical polarized micrographs of a) **1a** at 180 °C, b) **1a** at 130 °C, c) **1b** at 175 °C, d) **1b** at 130 °C, e) **1c** at 180 °C, and f) **1c** at 130 °C during the cooling process (magnification: ×100).

The thermal properties and LC behaviors of **1a-c** were investigated by thermogravimetric analyses (TGA), DSC, OPM, and small-angle X-ray scattering (SAXS). TGA analyses reveal that all these hybrids are thermally stable up to 220 °C (Fig. S13). DSC analyses of **1a-c** show that a glass transition state exists in all these hybrids during the heating and cooling process (Fig. S14). Specific exothermic and endothermic peaks, indicating the existence of liquid-crystalline phases, can be observed in the DSC curves of all the compounds except for **1a** (Table S1). However, all of them exhibit clear birefringence as observed by OPM measurements when directly cooling from isotropic state (Fig. 2 and S15). For **1a**, a typical fan-shaped texture, which can be assigned to a layered smectic A (SmA) phase, was obtained when cooling from isotropic state. Further decrease of temperature causes no significant change in texture until a frozen glass state appears. Similar situation can be observed for compounds **1b** and **1c**. However, some differences still exist. For example, during the cooling process of compound **1b** or **1c**, the fan-shaped texture gradually transfers to an irregular texture, indicating the thermal changes in enthalpy, which is in good accordance with the DSC measurements. These enthalpy changes, however, do not lead to phase transitions as revealed by the following SAXS studies.

To gain more insights on the arrangement of the molecules in the mesophase, variable-temperature SAXS measurements were carried out (Fig. 3). The SAXS patterns of **1a** shown in Fig. 3a are nearly independent of temperature (Table S5), and can be characterized by five reflexes at q = 1.12, 2.24, 3.41, 4.62, and 5.68 nm^{-1} with the ratio of 1:2:3:4:5, indicating a highly ordered lamellar structure. The interlayer distance d_{001} ($d_{001} = 2\pi/q_1$; 56.0 Å) is comparable with the molecular length in the extended molecular conformation (56.2 Å, calculated by MM2 force field method). This fact strongly suggests the existence of a lamellar SmA phase on cooling process. The SAXS patterns of **1b** and **1c** are almost the same with those of **1a**. Five equidistant reflexes are found in all temperature ranges (Fig. 3b and 3c). The interlayer distances (d_{001}) of **1b** and **1c** are calculated to be 59.1 Å and 62.2 Å, respectively, which are very close to the extended molecular lengths (59.0 Å for **1b** and 61.6 Å for **1c**). The interlayer distances of **1b** and **1c** determined by SAXS are also found to be nearly independent of temperature, which is in agreement with the nature of the SmA phase.[13] The reflex (q = 5.06 nm^{-1}) shown in all SAXS patterns corresponds to a distance of d' = 12.4 Å, presumably caused by neighboring POM clusters.[14,15]

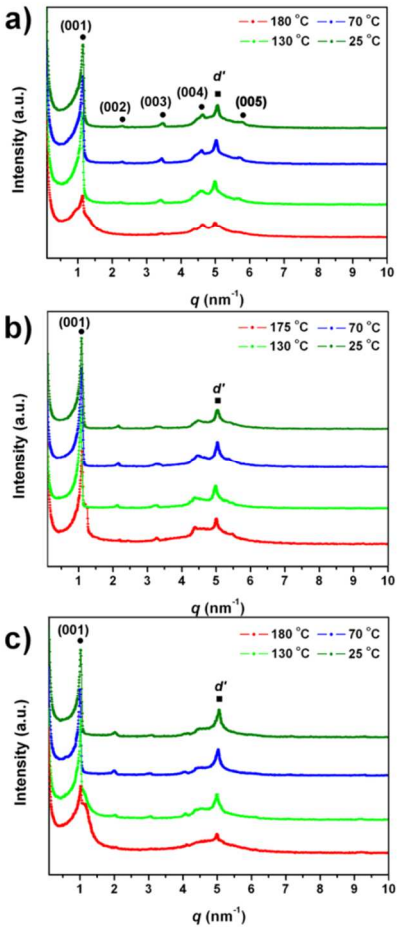

Fig. 3 Variable-temperature small-angle X-ray scattering patterns of a) **1a**, b) **1b**, and c) **1c** on cooling process.

We also employed TEM measurements to confirm the lamellar structures of **1a-c**. It can be seen clearly that the alternating patterns of the bright and dark streaks correspond to the gallic acid derivatives and POM clusters, respectively (Fig. S18). The lamellar distances are estimated to be 5.7, 6.0, and 6.2 nm for **1a**, **1b**, and **1c**, respectively, which are consistent with the interlayer distances obtained in the SAXS characterization. As the interlayer distances measured by SAXS and TEM are both nearly the same with the fully extended molecular lengths, the molecules are assumed to be oriented in a head-to-tail fashion[13,14] within the smectic layers and the alkyl chains are deeply interdigitated for efficient space filling. This proposed model is further confirmed

by HR-TEM. As shown in Fig 4b, well-ordered POM clusters within the POM-containing layer can be observed. On the basis of the above results, we propose a model for the packing structures of SmA phase (Fig. 4c), in which the organic moieties are located in between the POMs layers.

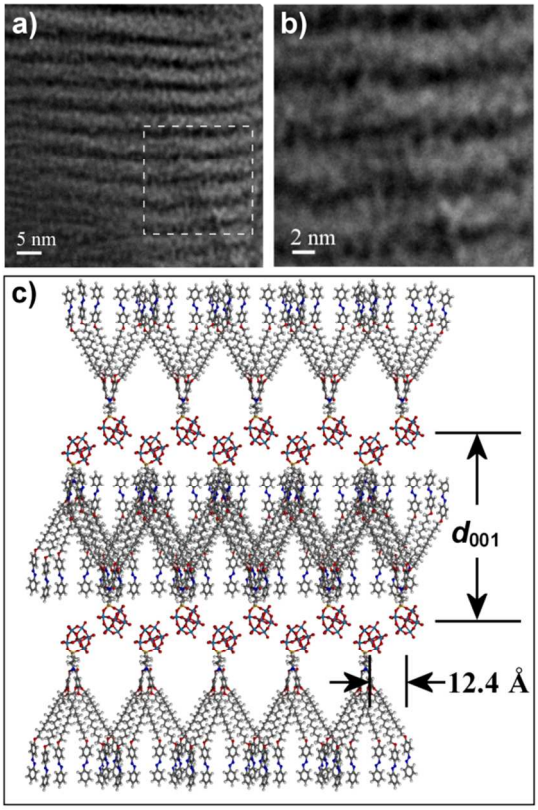

Fig. 4 a) HR-TEM image of **1c**; b) magnified HR-TEM image of **1c**; c) the suggested model describing the lamellar SmA structure.

Conclusions

In conclusion, we reported for the first time the synthesis and characterization of covalently modified POMs-containing thermotropic liquid-crystalline nanomaterials, in which the nonmesogenic organic moieties were tethered onto the nanoscaled POM cluster. These hybrids were found to be able to self-organize into a well-defined smectic lamellar structure, as confirmed by SAXS and HR-TEM measurements. Combining the advantages of organic moieties and tremendous properties of POMs, these hybrids allow the development of promising LCs in the field of smart multi-responsive material and catalyst. As such, this work provides fascinating perspectives in the design and elaboration of novel POMs-containing liquid-crystalline nanomaterials and may open a new pathway in the development of POMs-containing multifunctional nanosystems.

This research was supported by National Basic Research Program of China (973 program, 2014CB932104), National Science Foundation of China (21222104), the Fundamental Research Funds for the Central Universities (RC1302), Changjiang Scholars and Innovative Research Team in University. The authors appreciate the financial support from Beijing Engineering Center for Hierarchical Catalysts.

Notes and references

[a] *State Key Laboratory of Chemical Resource Engineering, Beijing University of Chemical Technology, Beijing 100029, P. R. China. E-mail: songyufei@hotmail.com, songyf@mail.buct.edu.cn; Fax: (+86) 10-64431832*

† Electronic Supplementary Information (ESI) available: Synthetic procedures; NMR, FT-IR, and ESI-MS spectra; TGA, DSC, OPM, and TEM. See DOI: 10.1039/b000000x/

1 D. Demus, J. W. Goodby, G. W. Gray, H.-W. Spiess, and V. Vill, *Handbook of Liquid Crystals*, Wiley-VCH, Weinheim, Germany, 1998.

2 T. Kato, N. Mizoshita and K. Kishimoto, *Angew. Chem. Int. Ed.*, 2006, **45**, 38; J. W. Goodby, I. M. Saez, S. J. Cowling, V. Gortz, M. Draper, A. W. Hall, S. Sia, G. Cosquer, S.-E. Lee and E. P. Raynes, *Angew. Chem. Int. Ed.*, 2008, **47**, 2754; C. Tshierske, *Chem. Soc. Rev.*, 2007, **36**, 193; B. Donnio, S. Buathong, I. Bury, and D. Guillon, *Chem. Soc. Rev.*, 2007, **36**, 1495.

3 H. Krishna, and S. Kumar, *Chem. Soc. Rev.*, 2011, **40**, 306.

4 T. Hegmann, and H. Qi, *J. Mater. Chem.*, 2006, **16**, 4197; T. Hegmann, H. Qi and V. M. Marx, *J. Inorg. Organomet. Polym. Mater.*, 2007, **17**, 483.

5 D.-L. Long, R. Tsunashima, and L. Cronin, *Angew. Chem. Int. Ed.*, 2010, **49**, 1736; Y.-F. Song, and R. Tsunashima, *Chem. Soc. Rev.*, 2012, **41**, 7384; H. N. Miras, J. Yan, D.-L. Long, and L. Cronin, *Chem. Soc. Rev.*, 2012, **41**, 7403; S.-T. Zheng, and G.-Y. Yang, *Chem. Soc. Rev.*, 2012, **41**, 7623; B. Hasenknopf, *Front. Biosci.*, 2005, **10**, 275; C. L. Hill, *Chem. Rev.*, 1998, **98**, 1; S. Omwoma, W. Chen, R. Tsunashima, and Y.-F. Song, *Coord. Chem. Rev.*, 2014, **258-259**, 58.

6 S. Polarz, B. Smarsly and M. Antonietti, *ChemPhysChem*., 2001, **7**, 457; T. Zhang, C. Spitz, M. Antonietti, and C. F. J. Faul, *Chem. Eur. J.*, 2005, **11**, 1001; T. Zhang, S. Liu, D. G. Kurth, and C. F. J. Faul, *Adv. Funct. Mater.*, 2009, **19**, 642.

7 W. Li, S. Yin, J. Wang, and L. Wu, *Chem. Mater.*, 2008, **20**, 514; Y. Jiang, S. Liu, S. Li, J. Miao, J. Zhang and L. Wu, *Chem. Commun.*, 2011, **47**, 10287; Y. Jia, H.-Q. Tan, Z.-M. Zhang, and E.-B. Wang, *J. Mater. Chem. C*, 2013, **1**, 3681.

8 S. Landsmann, C. Lizandara-Pueyo, and S. Polarz, *J. Am. Chem. Soc.*, 2010, **132**, 5315; S. Landsmann, M. Wessig, M. Schmid, H. Cölfen, and S. Polarz, *Angew. Chem. Int. Ed.*, 2012, **51**, 5995.

9 A. Proust, B. Matt, R. Villanneau, G. Guillemot, P. Gouzerh, and G. Izzet, *Chem. Soc. Rev.*, 2012, **41**, 7605; A. Dolbecq, E. Dumas, C. R. Mayer, and P. Mialane, *Chem. Rev.*, 2010, **110**, 6009;

10 E. Terazzi, C. Bourgogne, R. Welter, J.-L. Gallani, D. Guillon, G. Rogez, and B. Donnio, *Angew. Chem. Int. Ed.*, 2008, **47**, 490; E. Terazzi, G. Rogez, J.-L. Gallani, and B. Donnio, *J. Am. Chem. Soc.*, 2013, **135**, 2708.

11 Y. Molard, F. Dorson, V. Cîrcu, T. Roisnel, F. Artzner, and S. Cordier, *Angew. Chem. Int. Ed.*, 2010, **49**, 3351; A. S. Mocanu, M. Amela-Cortes, Y. Molard, V. Cîrcu, and S. Cordier, *Chem. Commun.*, 2011, **47**, 2056.

12 R. Deschenaux, B. Donnio, and D. Guillon, *New. J. Chem.*, 2007, **31**, 1064.

13 S. Campidelli, J. Lenoble, J. Barberá, F. Paolucci, M. Marcaccio, D. Paolucci, and R. Deschenaux, *Macromolecules*, 2005, **38**, 7915.

14 M.-B. Hu, Z.-Y. Hou, W.-Q. Hao, Y. Xiao, W. Yu, C. Ma, L.-J. Ren, P. Zheng, and W. Wang, *Langmuir*, 2013, **29**, 5714.

15 T. Nakanishi, T. Michinobu, K. Yoshida, N. Shirahata, K. Ariga, H. Möhwald, and D. G. Kurth, *Adv. Mater.*, 2008, **20**, 443.

Covalently Grafting Nonmesogenic Moieties onto Polyoxometalate for Fabrication of Thermotropic Liquid-Crystalline Nanomaterials

Chang-Gen Lin, Wei Chen, Solomon Omwoma, and Yu-Fei Song*

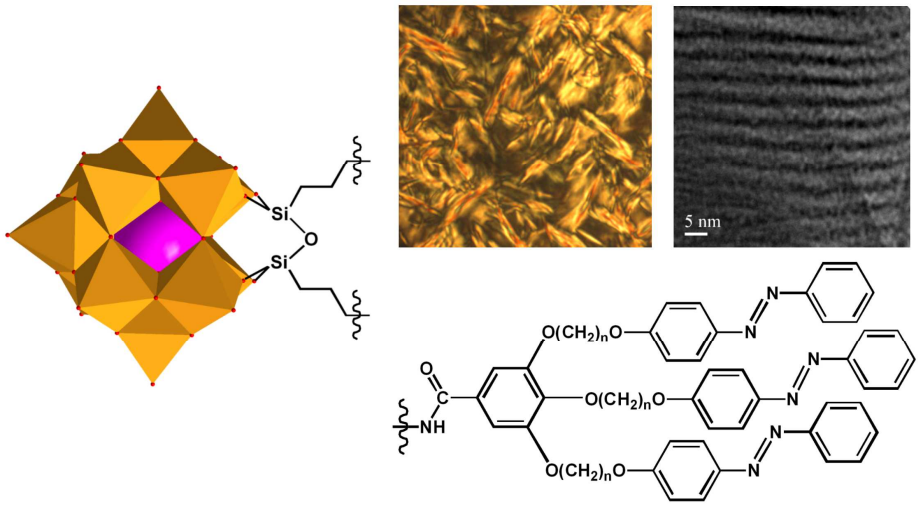

We demonstrated the first class of polyoxometalate-containing thermotropic liquid-crystalline materials constructed from nonmesogenic moieties.